

Reverse Myocardial Remodeling Following Valve Replacement in Patients With Aortic Stenosis



Thomas A. Treibel, PhD,^{a,b} Rebecca Kozor, MD,^a Rebecca Schofield, MBBS,^a Giulia Benedetti, MD,^a Marianna Fontana, PhD,^b Anish N. Bhuva, MBBS,^{a,b} Amir Sheikh, MD,^a Begoña López, PhD,^{c,d,e} Arantxa González, PhD,^{c,d,e} Charlotte Manisty, PhD,^{a,b} Guy Lloyd, MD,^{a,b} Peter Kellman, PhD,^f Javier Díez, MD, PhD,^{c,d,e,g} James C. Moon, MD^{a,b}

ABSTRACT

BACKGROUND Left ventricular (LV) hypertrophy, a key process in human cardiac disease, results from cellular (hypertrophy) and extracellular matrix expansion (interstitial fibrosis).

OBJECTIVES This study sought to investigate whether human myocardial interstitial fibrosis in aortic stenosis (AS) is plastic and can regress.

METHODS Patients with symptomatic, severe AS ($n = 181$; aortic valve area index $0.4 \pm 0.1 \text{ cm}^2/\text{m}^2$) were assessed pre-aortic valve replacement (AVR) by echocardiography (AS severity, diastology), cardiovascular magnetic resonance (CMR) (for volumes, function, and focal or diffuse fibrosis), biomarkers (N-terminal pro-B-type natriuretic peptide and high-sensitivity troponin T), and the 6-min walk test. CMR was used to measure the extracellular volume fraction (ECV), thereby deriving matrix volume ($\text{LV mass} \times \text{ECV}$) and cell volume ($\text{LV mass} \times [1 - \text{ECV}]$). Biopsy excluded occult bystander disease. Assessment was repeated at 1 year post-AVR.

RESULTS At 1 year post-AVR in 116 pacemaker-free survivors (age 70 ± 10 years; 54% male), mean valve gradient had improved ($48 \pm 16 \text{ mm Hg}$ to $12 \pm 6 \text{ mm Hg}$; $p < 0.001$), and indexed LV mass had regressed by 19% ($88 \pm 26 \text{ g/m}^2$ to $71 \pm 19 \text{ g/m}^2$; $p < 0.001$). Focal fibrosis by CMR late gadolinium enhancement did not change, but ECV increased ($28.2 \pm 2.9\%$ to $29.9 \pm 4.0\%$; $p < 0.001$): this was the result of a 16% reduction in matrix volume ($25 \pm 9 \text{ ml/m}^2$ to $21 \pm 7 \text{ ml/m}^2$; $p < 0.001$) but a proportionally greater 22% reduction in cell volume ($64 \pm 18 \text{ ml/m}^2$ to $50 \pm 13 \text{ ml/m}^2$; $p < 0.001$). These changes were accompanied by improvement in diastolic function, N-terminal pro-B-type natriuretic peptide, 6-min walk test results, and New York Heart Association functional class.

CONCLUSIONS Post-AVR, focal fibrosis does not resolve, but diffuse fibrosis and myocardial cellular hypertrophy regress. Regression is accompanied by structural and functional improvements suggesting that human diffuse fibrosis is plastic, measurable by CMR and a potential therapeutic target. (Regression of Myocardial Fibrosis After Aortic Valve Replacement; [NCT02174471](https://clinicaltrials.gov/ct2/show/study/NCT02174471)) (J Am Coll Cardiol 2018;71:860-71) © 2018 The Authors. Published by Elsevier on behalf of the American College of Cardiology Foundation. This is an open access article under the CC BY-NC-ND license (<http://creativecommons.org/licenses/by-nc-nd/4.0/>).



Listen to this manuscript's audio summary by JACC Editor-in-Chief Dr. Valentin Fuster.



From the ^aBarts Heart Centre, St. Bartholomew's Hospital, London, United Kingdom; ^bInstitute for Cardiovascular Sciences, University College London, London, United Kingdom; ^cProgram of Cardiovascular Diseases, Center for Applied Medical Research, University of Navarra, Pamplona, Spain; ^dInstituto de Investigación Sanitaria de Navarra (IdiSNA), Pamplona, Spain; ^eCardiovascular Biomedical Research Center Network (CIBERCV), Carlos III National Institute of Health, Madrid, Spain; ^fNational Heart, Lung, and Blood Institute, National Institutes of Health, Department of Health and Human Services, Bethesda, Maryland; and the ^gDepartment of Cardiology and Cardiac Surgery, University of Navarra Clinic, Pamplona, Spain. This project was funded by the National Institute of Health Research (NIHR) and European Commission FP7 Programme, Brussels, Belgium (FIBRO-TARGETS project 2013-602904). Dr. Treibel was supported by a doctoral research fellowship from the National Institute of Health Research (NIHR) (DRF-2013-06-102). Dr. Fontana was supported by a doctoral research fellowship from the British Heart Foundation (FS/12/56/29723). Dr. Moon is directly and indirectly supported by the University College London Hospitals NIHR Biomedical Research Centre. Dr. Manisty is directly and indirectly supported by the Biomedical Research Unit at St. Bartholomew's Hospital. All other authors have reported that they have no relationships relevant to the contents of this paper to disclose.

Manuscript received September 6, 2017; revised manuscript received December 12, 2017, accepted December 12, 2017.

Aortic stenosis (AS) is the most common valve disease and a prototype model for afterload-induced heart failure (1,2). Progressive aortic valve stenosis affects the left ventricle, which adapts to reduce wall stress and maintains cardiac output. Macroscopic adaptations are detected as left ventricular (LV) hypertrophy (LVH), whereas microscopic changes are characterized by cardiomyocyte hypertrophy and extracellular matrix expansion, caused by both focal replacement fibrosis (scar) and reactive, interstitial diffuse myocardial fibrosis (3-8).

SEE PAGE 872

Following aortic valve replacement (AVR, surgical or transcatheter), LVH regresses by 20% to 30% by 1 year (9-11). Whether this regression is cellular or interstitial has until recently been difficult to differentiate because it requires paired biopsies for histological examination. Cardiac magnetic resonance (CMR) is established as a tool for quantification of focal fibrosis by late gadolinium enhancement (LGE), but with T₁ mapping CMR can now also measure diffuse fibrosis by quantifying the extracellular volume fraction (ECV). CMR with T₁ mapping differentiates between cellular (myocytes, fibroblast, endothelial, red blood cells) and extracellular (extracellular matrix, blood plasma) compartments (Central Illustration) (12-14), and it offers the opportunity to track dynamic changes in the cell and matrix compartments. In AS, outcome is predicted not only by the extent of LVH at baseline or its regression post-AVR (10,15-17), but also by focal fibrosis (using LGE) (3-5) and diffuse fibrosis (using ECV) (18,19). Histological studies show that myocardial fibrosis accompanies cellular hypertrophy (20), and limited invasive studies suggest that both may regress after AVR (21).

We aimed to demonstrate that human myocardial fibrosis is plastic and can regress after AVR and that this regression can be measured noninvasively.

METHODS

This prospective observational cohort study was conducted in patients with severe, symptomatic AS who underwent AVR between January 2012 and January 2015 in a single tertiary referral cardiac center, University College London Hospital NHS Trust, London, United Kingdom. The study was approved by the ethical committee of the U.K. National Research Ethics Service (07/H0715/101) and was registered with ClinicalTrials.gov (Regression of Myocardial Fibrosis After Aortic Valve Replacement; NCT02174471). The study conformed to the principles of the Helsinki Declaration, and all subjects gave written informed

consent. Patients were recruited before preoperative evaluation. Pre-AVR and post-AVR, the comprehensive assessment included clinical history, blood pressure, 6-min walk test (6MWT) (22), blood sampling (for high-sensitivity troponin T [hsTnT] and N-terminal pro-B-type natriuretic peptide [NT-proBNP]), electrocardiography, transthoracic echocardiography, and CMR using the same equipment. Inclusion criteria were adult patients with severe AS (2 or more of: aortic valve area <1 cm², peak pressure gradient >40 mm Hg, aortic valve velocity ratio <0.25) who were undergoing AVR with or without coronary artery bypass grafting. Exclusion criteria were pregnancy or breastfeeding, estimated glomerular filtration rate <30 ml/min/1.73 m², CMR-incompatible implanted devices, inability to complete the protocol, previous valve surgery, or greater than moderate valve disease other than AS. Overall, 48% of patients undergoing surgical AVR for severe AS at our institution were recruited (Figure 1).

MULTIMODALITY CARDIAC IMAGING. Echocardiography was used to assess diastolic parameters and valve area or velocities (with CMR for regurgitant volumes if needed). CMR cine imaging was used to assess LV structure and systolic function. CMR T₁ mapping and ECV were undertaken for myocardial tissue characterization. All analysis was performed by operators blinded to clinical parameters.

Echocardiography. Clinical transthoracic echocardiography was performed using a GE Vivid E9 system (GE Healthcare, Waukesha, Wisconsin) with a 4-MHz transducer, following the guidelines of the American Society of Echocardiography and the European Society of Echocardiography (23).

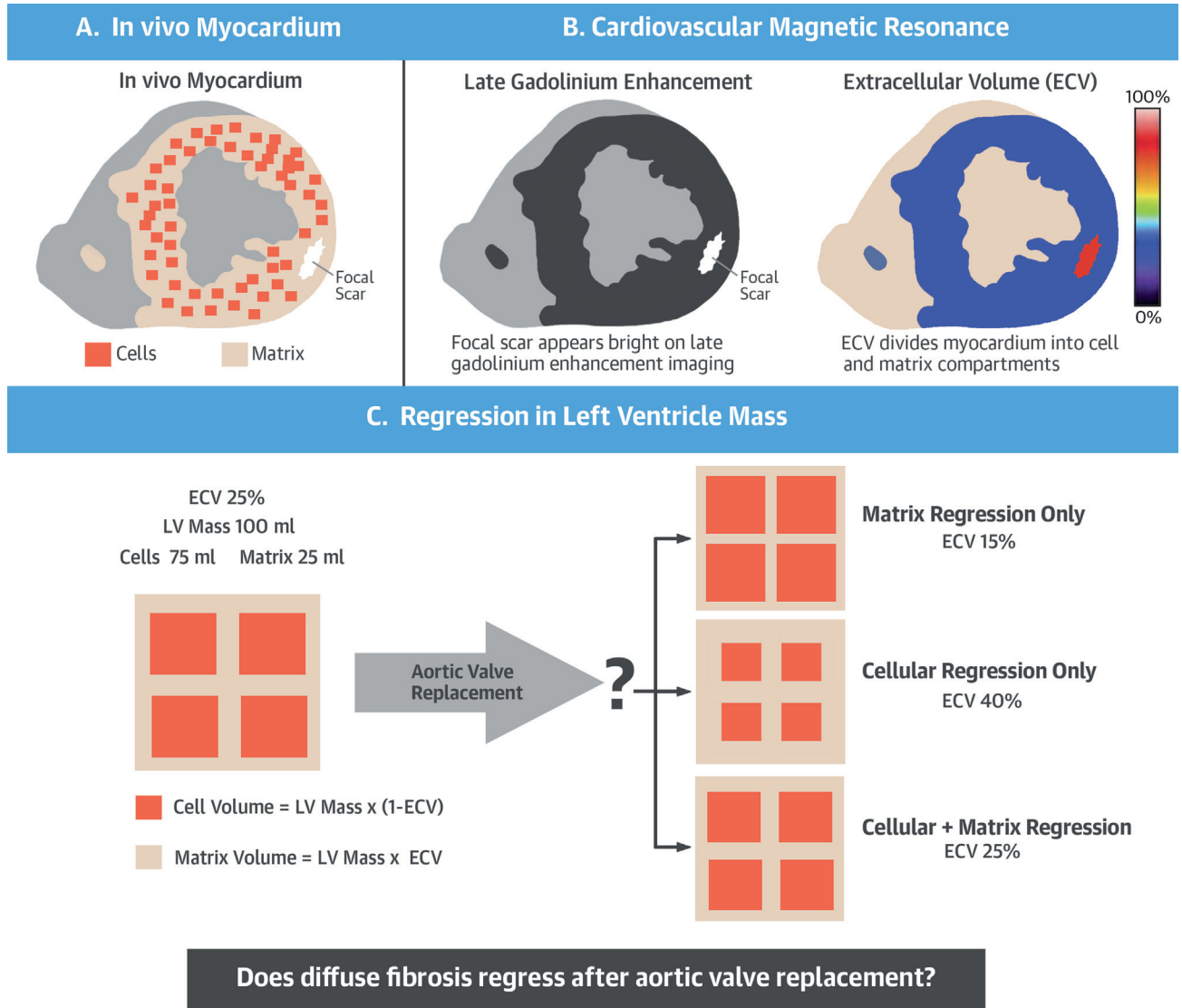
Cardiovascular magnetic resonance. CMR was performed at 1.5-T (Magnetom Avanto, Siemens Healthcare, Erlangen, Germany), by using a standard clinical scan protocol with late gadolinium enhancement (LGE) imaging and T₁ mapping (by Modified Look-Locker Inversion recovery [MOLLI]) (24) before and after a bolus of gadolinium contrast (0.1 mmol/kg of gadoterate meglumine [gadolinium-DOTA, marketed as Dotarem, Guerbet S.A., Paris, France]). Post-contrast imaging was performed at 10 min (LGE) and 15 min (T₁ mapping).

Imaging analysis. CMR image analysis was performed using CVI42 software (version 5.1.2[303],

ABBREVIATIONS AND ACRONYMS

6MWT	= 6-min walk test
AS	= aortic stenosis
AVR	= aortic valve replacement
CMR	= cardiovascular magnetic resonance
ECV	= extracellular volume fraction
hsTnT	= high-sensitivity troponin T
LGE	= late gadolinium enhancement
LV	= left ventricular
LVEF	= left ventricular ejection fraction
LVH	= left ventricular hypertrophy
LVM	= left ventricular mass
LVMI	= left ventricular mass index
NT-proBNP	= N-terminal pro-B-type natriuretic peptide
NYHA	= New York Heart Association

CENTRAL ILLUSTRATION Extracellular Volume Fraction Dichotomizes the Myocardium Into Cell and Matrix Compartments



Treibel, T.A. et al. *J Am Coll Cardiol.* 2018;71(8):860-71.

(A) The in vivo myocardium consists of cells and the surrounding extracellular matrix. Reactive fibrosis is characterized by expansion of the extracellular matrix, whereas replacement fibrosis follows cell death by focal scar. (B) Cardiovascular magnetic resonance measures both focal fibrosis (scar) by late gadolinium enhancement imaging, where the scar appears bright, and diffuse fibrosis by extracellular volume fraction (ECV) imaging. The ECV divides the myocardium into cell and matrix compartments and allows calculation of cell and matrix volumes. (C) A patient with a left ventricular (LV) volume of 100 ml and an ECV of 25% would have a cell volume of 75 ml and a matrix volume of 25 ml. Regression of left ventricular mass following aortic valve replacement can be driven by matrix regression alone, where the ECV reduces; by cellular regression alone, where the ECV increases; or by a proportional regression in cellular and matrix compartments, where the ECV is unchanged.

Circle Cardiovascular Imaging, Calgary, Alberta, Canada); myocardial mass by this method measures lower than by some other software platforms (25). LGE was assessed as a measurement of focal fibrosis,

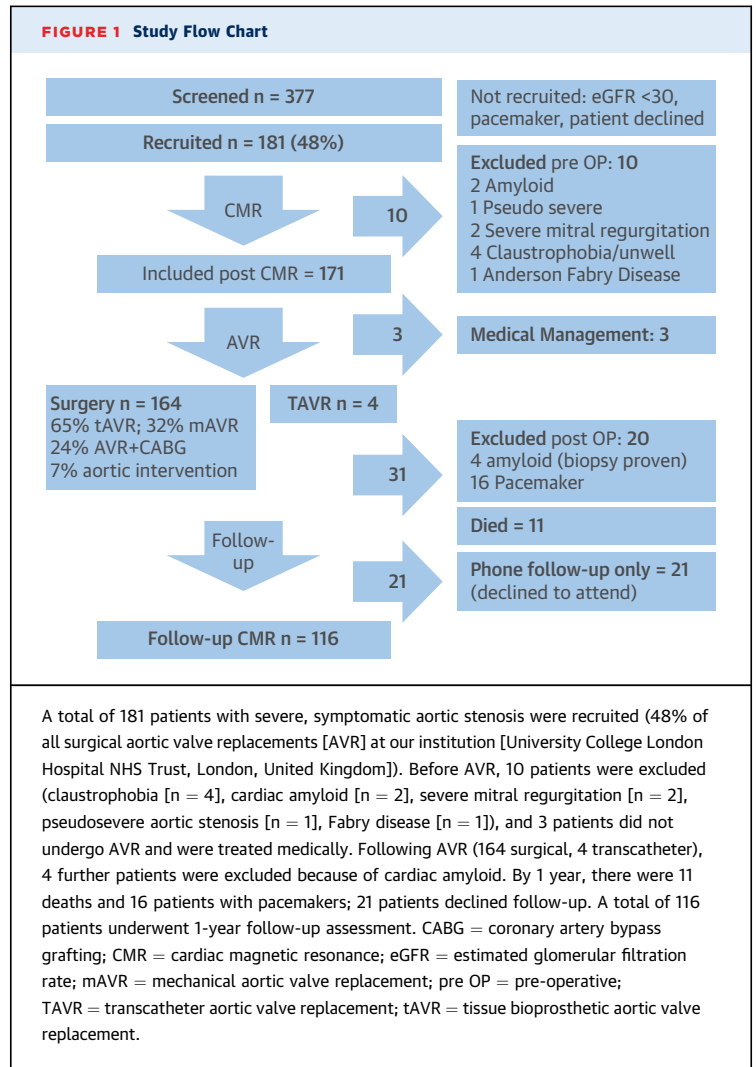
whereas ECV and matrix volume were used as measurements of diffuse myocardial fibrosis (Central Illustration). LGE was quantified from a short-axis LGE stack covering the extent of the left ventricle

by using a 3-SD threshold (Online Figure 1), and it was expressed in grams and as a percentage of the left ventricle. For T_1 mapping, 3 short-axis T_1 maps (base, middle, and apex) were manually contoured at the endocardial and epicardial border, segmented into an American Heart Association 16-segment model using the right ventricular insertion points. Partial voluming of blood was minimized by setting an automatic offset of 10% from the endocardial and epicardial borders. Segments with myocardial infarction (endocardial LGE) on LGE imaging were excluded. ECV was calculated as: $ECV = (1 - \text{hematocrit}) \times [\Delta R1_{\text{myocardium}}] / [\Delta R1_{\text{bloodpool}}]$ (26), where $\Delta R1$ is the difference in relaxation rates ($1 / T_1$) pre-contrast and post-contrast (13). Total LV matrix and cell volumes were calculated from the product of LV myocardial volume (LV mass [LVM] divided by the specific gravity of myocardium [1.05 g/ml]) and ECV or $(1 - ECV)$, respectively. Further details can be found in the Online Methods section.

STATISTICAL ANALYSIS. Statistical analyses were carried out using SPSS software version 22 (IBM, Armonk, New York). All continuous variables are expressed as mean \pm SD or median (interquartile range [IQR]) for skewed data. Normality was checked using the Shapiro-Wilk test. Categorical variables are expressed as percentages. Groups were compared using the independent-samples Student's *t*-test for normally distributed continuous variables, the Mann-Whitney *U* test for non-normally distributed variables, and the Fisher exact test or a chi-square test for categorical variables. Changes between pre-AVR and post-AVR visits were compared using paired Student's *t*-tests for continuous variables and using Wilcoxon signed rank test for ordinal variables (New York Heart Association [NYHA]). Log transformation was applied to normalize the distribution of NT-proBNP and hsTnT. To identify predictors of LVM and matrix regression, all clinical parameters were proposed for inclusion in a univariate linear regression model, and the most significant predictors per domain were then entered into a stepwise multivariable model to identify significant independent predictors. A 2-sided *p* value of <0.05 was considered significant.

RESULTS

STUDY POPULATION. A total of 181 patients with severe, symptomatic AS (age 69 ± 10 years; 56% male) were recruited. Three patients did not undergo AVR and were treated medically. Following AVR, 14 patients were excluded (cardiac amyloid [$n = 6$] (27), claustrophobia [$n = 4$], severe mitral regurgitation [$n = 2$], pseudosevere AS [$n = 1$], Fabry disease [$n = 1$]).



By 1 year, there were 11 deaths and 16 patients with pacemakers; 21 patients declined follow-up. A total of 116 patients underwent 1-year follow-up assessment and were included in the analysis, as shown in the study flowchart (Figure 1). There was no significant difference in baseline characteristics between patients who completed the follow-up and those who did not, in particular with regard to age, sex, AS severity, or surgical risk score (all $p > 0.05$).

BASELINE FINDINGS. Baseline demographic, clinical, echocardiographic, and CMR characteristics of the follow-up study cohort ($n = 116$; age 70 ± 10 years of age; 54% male) are shown in Tables 1 and 2 (Online Table 1).

Valve stenosis severity. All patients had severe AS by echocardiography (aortic valve area index $0.40 \pm 0.13 \text{ cm}^2/\text{m}^2$; mean gradient $48 \pm 14 \text{ mm Hg}$; peak

TABLE 1 Baseline Clinical Characteristics (N = 116)	
Age, yrs	70 ± 10
Male	63 (54)
Trileaflet	83 (72)
Bicuspid*	33 (28)
BSA, m ²	1.90 ± 0.22
Comorbidities	
Hypertension	87 (75)
SBP, mm Hg	133 ± 17
DBP, mm Hg	76 ± 10
Diabetes	23 (20)
Coronary artery disease	34 (29)
Atrial fibrillation	16 (14)
Risk scores	
STS, %	1.3 (1.0-2.1)
EuroSCORE II, %	1.4 (1.0-2.4)
Drug history	
ACE inhibitor/ARB	51 (44)
Beta-blocker	43 (37)
Statin	74 (64)
Aspirin	51 (44)
Blood	
Creatinine, μmol/l	85 ± 26
eGFR, ml/min/1.73 m ²	77 ± 21
Hematocrit, %	40.4 ± 4.5
Histology	
Collagen volume fraction, %†	7.7 (4.2-12.7)
Values are mean ± SD, n (%), or median (interquartile range). *One patient had unicuspid aortic stenosis (female). †n = 91. ACE = angiotensin-converting-enzyme; ARB = angiotensin receptor blocker; BSA = body surface area; DBP = diastolic blood pressure; eGFR = estimated glomerular filtration rate; EuroSCORE II = European System for Cardiac Operative Risk Evaluation II score; IQR = interquartile range; LVH = left ventricular hypertrophy; NYHA = New York Heart Association; SBP = systolic blood pressure; STS = The Society of Thoracic Surgeons risk model score.	

velocity 4.4 ± 0.6 m/s). The etiology of AS was determined as calcific AS (n = 83; 72 ± 8 years of age; 52% male), bicuspid AS (n = 32; 59 ± 6 years of age; 66% male), and unicuspid AS (n = 1; 1 35-year-old female patient) by a combination of echocardiography, CMR, and direct inspection during surgery.

Symptoms and functional capacity. All but 7 patients were symptomatic (94%), with dyspnea (95%), chest pain (32%), and/or syncope (8%). Median 6MWT distance was 500 m (IQR: 390 to 600 m).

INTERVENTION. The interval between CMR and AVR was a median of 33 days (IQR: 6 to 62 days). AVR was carried out using cardiopulmonary bypass with blood cardioplegia arrest. The valve received was a tissue (n = 103; 61%), sutureless (n = 7; 4%), or mechanical valve (n = 54; 32%), with additional bypass grafting in 30 patients (24%) and intervention on the aorta in 11 (7%; interposition graft, reduction aortoplasty, replacement of the ascending aorta). Mean bypass and

cross-clamp times were 91 ± 26 min and 72 ± 25 min, respectively. Four patients initially referred for surgical valve replacement underwent transcatheter AVR after review by the heart valve team and were included in the final analysis. Perioperative myocardial biopsies (n = 91) were analyzed for collagen volume fraction (median 7.7%; IQR: 4.2% to 12.7%).

LEFT VENTRICULAR REMODELING AT 1 YEAR AFTER AVR. At 1 year post-AVR, there was a marked improvement in aortic valve obstruction (mean gradient 48 ± 16 mm Hg to 12 ± 6 mm Hg; peak gradient 77 ± 20 mm Hg to 24 ± 11 mm Hg; both $p < 0.001$) and LV afterload (valvuloarterial impedance index 4.3 ± 1.2 mm Hg/ml/m² to 3.6 ± 0.9 mm Hg/ml/m²). The changes from pre-operative to post-operative parameters are summarized in [Table 2](#).

There was a 19% reduction in indexed LVM (88 ± 26 g/m² to 71 ± 19 g/m²; $p < 0.001$) ([Figure 2A](#)), as well as a reduction in LV end-diastolic volume index and LV end-systolic volume index, resulting in a reduction in the mass-to-volume ratio. LV ejection fraction (LVEF) increased modestly ($71 \pm 16\%$ to $74 \pm 12\%$; $p < 0.006$). LVM regression occurred regardless of the baseline level of hypertrophy (i.e., also in patients with normal geometry), although both absolute and percentage of LVM index (LVMI) regression were greatest in those patients with the highest LVMI at baseline ([Online Figure 2](#)). On multivariate regression analysis, high baseline LVMI, elevated baseline NT-proBNP level, and lower baseline LVEF were independently associated with greater LVMI regression ([Table 3](#)) (post-operative change in mean aortic valve gradient did not reach significance [$p = 0.06$]).

MYOCARDIAL FIBROSIS AT 1 YEAR AFTER AVR. ECV increased from $28.2 \pm 2.9\%$ to $29.9 \pm 4.0\%$ ($p < 0.001$) ([Figure 2B](#)); as a result, derived cell volume reduced by 22% (14.0 ± 11.6 ml/m²) from 64 ± 18 ml/m² to 50 ± 13 ml/m² ($p < 0.001$) ([Figure 2C](#)), and derived matrix volume reduced by 16% (4.1 ± 5.8 ml/m²) from 25 ± 9 ml/m² to 21 ± 7 ml/m² ($p < 0.001$) ([Figure 2D](#)). Native myocardial T₁ was unchanged ($1,039 \pm 40$ ms vs. $1,035 \pm 42$ ms; $p = 0.3$). Focal fibrosis in absolute terms (LGE in g/m²) did not change at follow-up (6.4 ± 4.9 g/m² vs. 6.5 ± 4.4 g/m²; $p = 0.9$), but expressed as a percentage of the regressed LVM, focal fibrosis (LGE as %) increased post-AVR ($7.2 \pm 5.1\%$ vs. $8.9 \pm 4.9\%$; $p = 0.001$). There were no differences in ECV, cell, or matrix volume changes according to coronary artery disease status, although patients with coronary artery disease had higher hsTnT levels and focal fibrosis ([Online Tables 2 and 3](#)). Matrix regression was greatest in those patients with the highest

TABLE 2 Changes After Aortic Valve Replacement (N = 116)

	Pre-AVR	Post-AVR	Change	p Value
NYHA functional class				
I	15 (13)	70 (60)	+55 (+47)	<0.001
II	59 (51)	41 (35)	-18 (-15)	
III	40 (34)	5 (5)	-35 (-30)	
IV	2 (2)	0	-2 (-2)	
6-min walk test, m	477 ± 177*	571 ± 171	+90 (0 to +180)	<0.001
NT-proBNP, ng/l	50 (26-173)	38 (23-99)	-14 (-67 to +9)	<0.001
hsTnT, pmol/l	13 (9-20)	11 (7-17)	-1 (-4 to +1)	0.002
Echocardiography				
Vmax, m/s	4.4 ± 0.6	2.4 ± 0.5	-2.1 ± 0.8	<0.001
Peak gradient, mm Hg	77 ± 20	24 ± 11	-53 ± 22	<0.001
Mean gradient, mm Hg	48 ± 14	13 ± 6	-35 ± 16	<0.001
EOAI, cm ² /m ²	0.40 ± 0.13	0.84 ± 0.21	+0.45 ± 0.25	<0.001
LVOT-to-aortic valve VTI ratio	0.23 ± 0.08	0.51 ± 0.12	+0.28 ± 0.13	<0.001
Zva, mm Hg/ml/m ²	4.3 ± 1.2	3.6 ± 0.9	-0.8 ± 1.2	<0.001
E-wave, m/s	0.83 ± 0.29	0.83 ± 0.23	+0.06 (0.20 to -0.14)	0.20
E/A ratio	0.94 ± 0.49	0.91 ± 0.26	-0.06 (-0.30 to +0.17)	0.60
E deceleration time, ms	234 ± 72	242 ± 67	+12 (-69 to +65)	0.70
Mean E/e' ratio	13.2 ± 5.8	10.8 ± 4.2	-1.1 (-5.4 to +1.9)	0.001
LVRPP, mm Hg × beats/min	15,172 ± 2,924	11,140 ± 2,166	-3,805 (-1,881 to -6,176)	<0.001
CMR parameters				
LVEDVI, ml/m ²	66 ± 23	62 ± 19	-2 (-12 to +8)	0.03
LVESVI, ml/m ²	22 ± 21	18 ± 13	-7 (-35 to +31)	0.003
LVEF, %	71 ± 16	74 ± 12	+1 (-5 to +10)	0.006
LVMI, g/m ²	88 ± 26	71 ± 19	-18 (-22 to -11)	<0.001
Mass-to-volume ratio	1.42 ± 0.37	1.19 ± 0.27	-0.22 (-0.40 to -0.05)	<0.001
LAAI, cm ² /m ²	13.2 ± 3.0	12.1 ± 2.2	-0.5 (-1.2 to +0.9)	0.09
Tissue characterization				
LGE 3SD method, g/m ²	6.4 ± 4.9	6.5 ± 4.4	0 (-2.3 to +2.0)	0.90
LGE 3SD method, %	7.2 ± 5.1	8.9 ± 4.9	+2 (-10 to +12)	0.001
T1 myocardium (native), ms	1,039 ± 40	1,035 ± 42	-11 (-36 to +26)	0.30
ECV, %	28.2 ± 2.9	29.9 ± 4.0	+1.2 (+3.4 to -0.5)	<0.001
Cell volume, indexed, ml/m ²	64 ± 18	50 ± 13	-14.0 (-19.2 to -6.3)	<0.001
Matrix volume, indexed, ml/m ²	25 ± 9	21 ± 7	-3.5 (-6.8 to -0.8)	<0.001

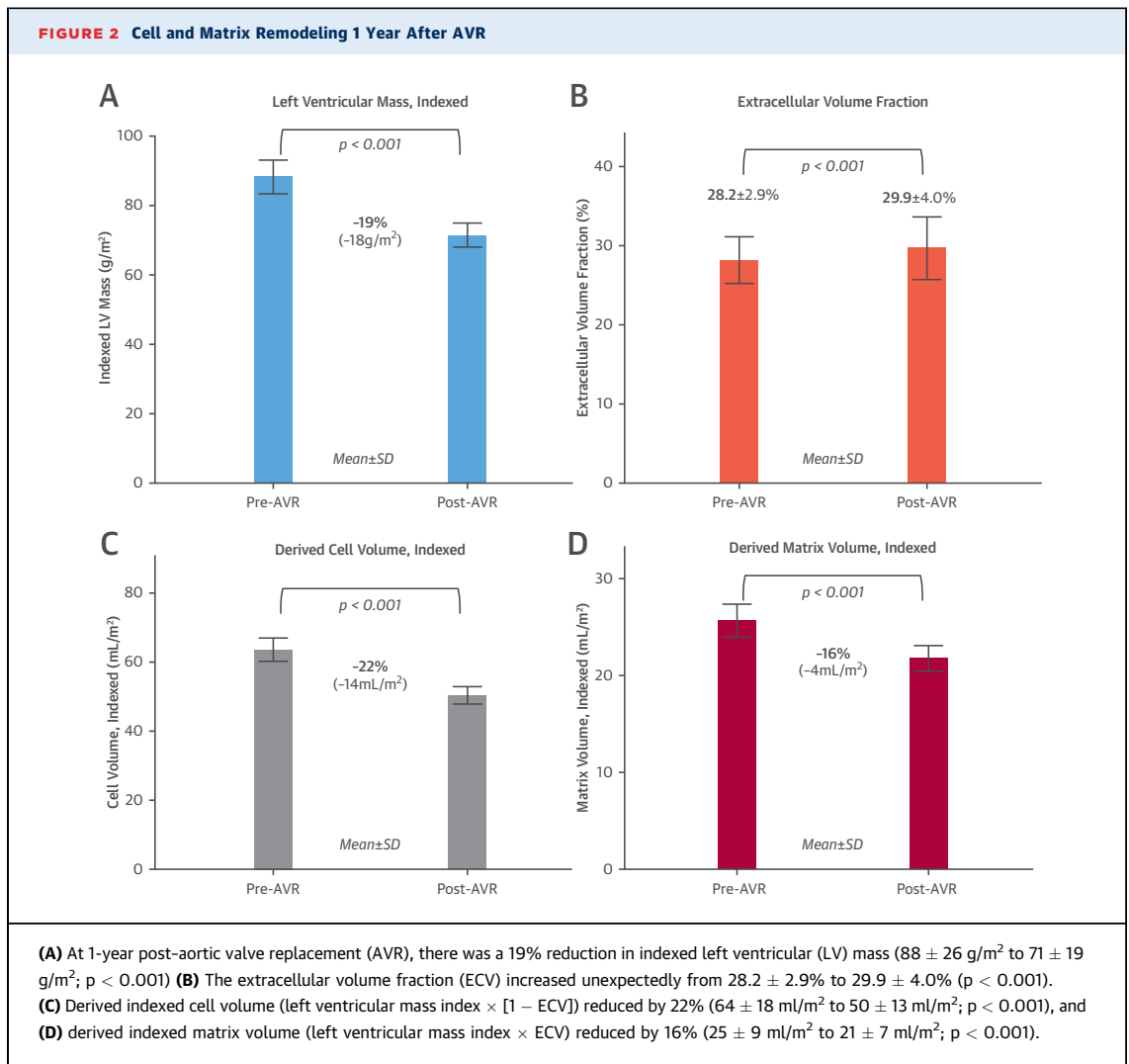
Values are n (%), median (interquartile range), or mean ± SD. **Bold** p values are statistically significant. *n = 85.

3SD = 3 SDs; AVAI = aortic valve area index; AVR = aortic valve replacement; CMR = cardiac magnetic resonance; DT = deceleration time; E = peak early velocity of the transmitral flow; E/A ratio = ratio of early to late ventricular filling velocities; E' = peak early diastolic velocity of the mitral annulus displacement; ECV = extracellular volume fraction; EOAI = effective orifice area index; hsTnT = high-sensitivity troponin T; LAAI = left atrial area index; LGE = late gadolinium enhancement; LVEDVI = left ventricular end-diastolic volume index; LVEF = left ventricular ejection fraction; LVESVI = left ventricular end-systolic volume index; LVMI = left ventricular mass index; LVOT = left ventricular outflow tract; LVRPP = left ventricular rate pressure product; NT-proBNP = N-terminal pro-B-type natriuretic peptide; NYHA = New York Heart Association; SVI = stroke volume index; Vmax = peak velocity through the aortic valve; VTI = velocity-time integral; Zva = valvuloarterial impedance.

matrix volume at baseline (Online Figure 3). On univariate regression analysis, matrix regression was associated with baseline LV parameters (LV size, hypertrophy, systolic and diastolic function), baseline biomarkers (hsTnT and NT-proBNP), and post-operative changes in valve hemodynamics (Online Table 4). On multivariate analysis, high baseline LVMI, elevated baseline NT-proBNP level, and high baseline ECV were independently associated with greater matrix volume regression (Table 3).

FUNCTIONAL IMPROVEMENT. One year after AVR, patients were less breathless (NYHA functional class

improved by nearly 1 class; p < 0.001) and could walk farther (6MWT improvement 90 m; p < 0.001). In addition, both left atrial pressure, reflected by a reduction in the E/e' ratio (13 ± 6 cm/s to 11 ± 4 cm/s; p = 0.003) and NT-proBNP levels were reduced (50 ng/l [IQR: 26 to 173 ng/l] to 38 ng/l [IQR: 23 to 99 ng/l]; p < 0.001). There were no significance differences in these parameters in patients undergoing isolated AVR versus patients undergoing AVR and coronary artery bypass grafting (Online Tables 2 and 3). On multivariate analysis, shorter baseline 6MWT distance and elevated systolic blood pressure were independently associated with greatest



improvements in NYHA functional class, as well as greatest improvements in 6MWT distance (Online Tables 5 and 6). Baseline parameters, AS severity, and biomarker (hsTnT or NT-proBNP) levels were not predictive of improvement in 6MWT distance.

DISCUSSION

In this study we sought to understand the dynamic nature of cellular and matrix components in myocardial hypertrophy by exploring reverse myocardial remodeling in AS at 1 year post-AVR. We show that myocardial cellular hypertrophy and extracellular matrix expansion (diffuse fibrosis) regress, and these changes are accompanied by structural, functional, and biomarker improvement.

Furthermore, the study establishes that cardiomyocyte loss is irreversible, as evidenced by the persistence of focal replacement fibrosis (LGE) after AVR. Moreover, these findings provide validation that CMR can be used to characterize and monitor the extent of cellular hypertrophy and myocardial fibrosis, thereby differentiating between focal fibrosis (scar) and diffuse fibrosis secondary to accumulation of ECM and, importantly, confirming myocardial fibrosis regression noninvasively, similar to that reported >25 years ago requiring invasive myocardial biopsies (28,29).

The concept of reverse myocardial remodeling after removal of a pathological insult has been studied both by echocardiography and by CMR. LVH (i.e., combined cell and matrix compartments) is known to

TABLE 3 Predictors of Change in Indexed Left Ventricular Mass and Indexed Matrix Volume After Aortic Valve Replacement

	Univariate Predictors			Multivariate Predictors*		
	Beta	95% CI	p Value	Beta	95% CI	p Value
Predictors of change in LVMI after AVR†						
Baseline LVMI, g/m ²	-0.4	-0.4 to -0.3	<0.001	-0.13	-0.23 to -0.04	0.004
Baseline NT-proBNP, ng/l	-0.06	-0.08 to -0.03	<0.001	-0.01	-0.02 to -0.01	0.01
LVEF, %	0.34	0.16 to 0.51	<0.001	0.23	0.01 to 0.45	0.04
Δ mean AV gradient, mm Hg	0.20	0.06 to 0.34	0.006	0.14	0.01 to 0.28	0.06
Age	0.24	0.01 to 0.47	0.04			NS
Systolic BP, mm Hg	0.40	0.01 to 0.7	0.04			NS
LGE, g	-0.7	-1.2 to -0.1	0.02			NS
ECV, %	-245	-442 to -48	0.02			NS
Prosthesis size	-3.66	-5.92 to -1.4	0.002			NS
Predictors of change in indexed matrix volume after AVR‡						
Baseline LVMI, g/m ²	-0.12	-0.15 to -0.08	<0.001	-0.82	-0.12 to -0.05	<0.001
Baseline NT-proBNP, ng/l	-0.01	-0.015 to -0.006	<0.001	-0.004	-0.008 to -0.001	0.03
ECV, %	-0.87	-1.19 to -0.56	<0.001	-34.8	-68.5 to -1.0	0.04
LVEF, %	0.14	0.07 to 0.20	<0.001			NS
Δ mean AV gradient, mm Hg	0.071	0.002 to 0.139	0.04			NS
Age	0.078	-0.034 to 0.191	0.20			NS
Male	-2.23	-4.40 to -0.62	0.04			NS
LGE, g	-0.12	-0.22 to -0.01	0.032			NS
E/A ratio	-3.99	-6.33 to -1.64	0.001			NS
hsTnT, pmol/l	-2.90	-4.47 to -1.34	<0.001			NS
Prosthesis size	-0.55	-0.97 to -0.12	0.012			NS
CVF, %	-0.13		0.40			NS

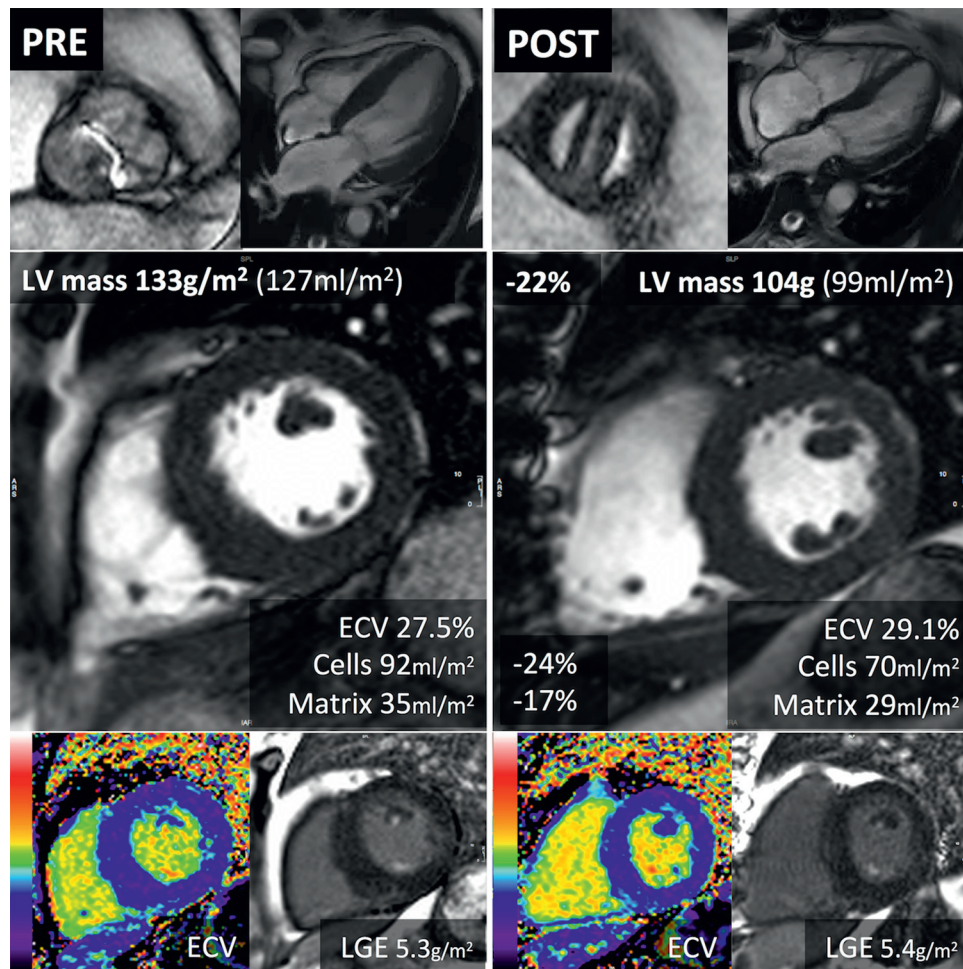
Bold p values are statistically significant. *Stepwise multivariate linear regression model. †LVMI at baseline minus LVMI at 1 year post-AVR. ‡Indexed matrix volume at baseline minus indexed matrix volume at 1 year post-AVR.
 Δ = change; AV = aortic valve; BP = blood pressure; CI = confidence interval; CVF = collagen volume fraction; LVMI regression = reduction in LVMI (negative); Matrix volume regression = reduction in matrix volume (negative). other abbreviations as in [Table 2](#).

regress by 20% to 30% by 1 year post-AVR (9-11). We now show that both cell regression and matrix regression contribute to the reduction in LVH over this period (Figure 3).

Combined with our previous data showing that at 6 months post-AVR only cellular hypertrophy regresses (30), this study suggests that the timeline for cardiomyocyte and extracellular matrix responses to afterload reduction are different, with remodeling of the extracellular matrix being slower. Diffuse fibrosis enhances myocardial tensile strength and 3-dimensional force delivery but at the expense of reduced distensibility. Dense collagen meshwork within the subendocardium seen in AS can be considered pathological in that it entraps muscle fibers and causes active stiffness to fall while impairing distensibility (31). This current work translates the biopsy findings from >30 years ago by Hans-Peter Kraysenbuehl and his group (29) into an era where AS is a different disease and non-invasive imaging by CMR offers in vivo whole heart myocardial tissue characterization. It is important

to recognize that the demographic features of patients with severe AS have dramatically changed over this period of time: First, the small cohort (n = 20 vs. n = 116) in the earlier study was younger and predominantly male (mean age 52 years; range 25 to 67 years; 35% women), in contrast to our cohort, which had a mean age 70 years, with 44% women. Second, advances in surgical technique have improved perioperative myocardial preservation, and advances in prosthesis technology offer better hemodynamic performance and valve durability.

Previous data by Villari et al. (21) suggested no change in interstitial fibrosis at 2 years post-AVR, but these data were from subendocardial samples rather than a global, “whole heart” measure as in our cohort. Location of the biopsy sample is crucial, as we have shown in previous work (32), where the subendocardial portion of the myocardium was dominated by replacement focal fibrosis decreasing from superficial to deep such that reactive fibrosis predominated in the midmyocardium.

FIGURE 3 Reverse Myocardial Remodeling After AVR

A 66-year-old man with severe aortic stenosis (peak velocity 4.66 m/s; mean gradient 57 mm Hg; aortic valve area 0.5 cm²). Cardiac magnetic resonance before aortic valve replacement (AVR) showed concentric left ventricular (LV) hypertrophy (133 g/m²). Late gadolinium enhancement (LGE) demonstrated limited nonischemic focal scar (5.3 g/m² [4%]). Extracellular volume fraction (ECV) was 27.5%. At 1 year after AVR (mechanical bileaflet valve), there was a 22% reduction in LV mass (to 104 g/m²). The LV mass regression resulted from a 24% reduction in cell volume and a 17% reduction in matrix volume, so the ECV rose to 29.1%. The focal fibrosis (late gadolinium enhancement [LGE]) was unchanged (5.4 g/m² [5%]), but it slightly increased when it was expressed as a percentage of the LV mass.

The ability to measure extracellular matrix regression noninvasively by CMR (as a surrogate for diffuse fibrosis) not only reflects a key biological response, but also has the potential to be used in drug development to validate proof-of-concept efficacy of drugs targeting myocardial fibrosis. The possibility of influencing myocardial (cellular and interstitial) remodeling with pharmacological interventions (33-35) requires a better understanding of the intricate interplay throughout all stages of disease. Noninvasive tracking of cellular and extracellular components may

potentially establish the transition point between adaptive and maladaptive remodeling and provide a reliable method to monitor the response to matrix-modulating therapies (antifibrotic, antiamyloid) in the search for new individualized heart failure therapies (36).

Native T₁ of the myocardium did not change post-AVR. The most likely explanation is that these 2 parameters capture different compartments: ECV captures the extracellular components of the myocardium, (e.g., extracellular matrix and vascular

spaces [capillaries]), whereas native T_1 is a composite signal of both the cellular and extracellular compartments.

Focal fibrosis identified by LGE is indicative of cardiomyocyte necrosis with replacement fibrosis (i.e., ranging from foci of necrosis to larger myocardial infarcts). Our data suggest that focal fibrosis, reflected by LGE, does not regress; this is consistent with previous findings reported post-AVR implying that AVR failed to reduce the degree of focal replacement fibrosis (6,37). In contrast, the reactive diffuse fibrosis did regress. These findings highlight the dynamic nature of the extracellular matrix in AS that contributes to the pathobiology because changes in collagen turnover occur as a result of the reaction of cardiac fibroblasts to both mechanical and local humoral factors (38,39). Matrix volume and fraction (ECV) quantification may add more predictive information, particularly given that our data clearly show that this method identifies measurable reversibility. This is also important from an outcome perspective because recent data by Chin et al. (19) showed that both focal fibrosis (LGE) and diffuse fibrosis (matrix volume) were univariate predictors of outcome.

Current management strategies for AS mainly rely on waiting until the onset of symptoms. However, it is recognized that for some patients this treatment is too late; furthermore, there is a discrepancy between symptom development and markers of long-term outcome post-AVR (e.g., LGE). This requires confirmation in asymptomatic patients; however, the recent PRIMID-AS (Prognostic Importance of Microvascular Dysfunction in Aortic Stenosis) study showed that LGE and ECV were not associated with symptom development (trend for ECV) (40).

Although existing models of AS may be simplistic, our current understanding is that AS is a disease of both the valve and the myocardium. Thus treatment strategies need to assess both the hemodynamic insult imposed by the valve lesion and the extent of myocardial structural remodeling, particularly when seeking to quantify irreversible changes and predict outcome. Reduced LVEF, excessive LVH, abnormal response to exercise, and critical AS (peak velocity >5 m/s) (15,41), as well as LGE (3-5), are markers for this and have been shown to predict adverse outcome. Although LVH regression occurs early post-AVR (42,43), myocardial normalization is not always possible. We show that focal replacement fibrosis is not plastic but

irreversible, which is not surprising, but it may represent a point in the clinical progression of AS at which valve replacement should be recommended to prevent further irreversible damage. If this transition point to maladaptive remodeling could be anticipated, then intervention could be performed before the emergence of irreversible focal replacement scar; a combination of blood and imaging biomarkers may be able to identify these transition points in the future. Finally, drug therapies could be used post-AVR to augment or accelerate normalization of both cell hypertrophy and diffuse fibrosis.

STUDY LIMITATIONS. There are limits to an exclusively noninvasive approach. The ECV technique is measuring extracellular water, which tracks fibrosis, but there are other explanations: vasodilation, edema, and amyloid. Compensatory capillary vasodilation (hyperemia) would cause elevated native myocardial T_1 and ECV (44). However, AS is believed to have a reduced capillary density (45), and the changes found here are too large for blood volume—16% of total myocardial volume. We also saw no predicted change in native T_1 . Edema could be a cause, which has been described in increased afterload (46). However, these patients had normal baseline myocardial T_2 . A dual pathological process with occult amyloid was specifically sought and excluded ($n = 6$), so it was not present (27). ECV quantification excluded infarct LGE but included nonischemic LGE, as per guideline recommendation (26). Although exclusion of all areas of LGE may appear theoretically attractive, it would be practically challenging to limit the ECV measurement area to exclude pixels of non-infarct LGE (highlighted by our thresholding method). Ultimately, the inclusion of areas of non-infarct LGE in the ECV measurement did not affect the overall regression trend because the amount of LGE did not change at follow-up. Although the lack of change in LGE area post-AVR may contribute to the ECV increase post-AVR, it will simultaneously lead to underestimation of the proportion of matrix regression. Previous studies (47) used cutoffs of ECV to predict the presence of LGE, but this approach would not be appropriate. We have shown recently that LGE and ECV increases probably reflect different mechanisms, and that technical aspects are important (32): whereas fibrosis elevates ECV, physiological cell hypertrophy lowers ECV (as seen in athletic hypertrophy [48]). LGE does not capture this cellular component.

Other limitations of the present study include that it is a single-center study and it focused on surgical AVR by noninvasive CMR assessment without paired histological examination. Pressures were determined by noninvasive, echocardiography-derived values only. Patients in renal failure or with pacemakers are not represented (this excluded 7% of possible patients). Some patients declined follow-up, but there was no significant difference in baseline characteristics between patients who completed the follow-up and those who withdrew.

CONCLUSIONS

In aortic stenosis following AVR, both cellular hypertrophy and diffuse fibrosis regress, and these changes are accompanied by structural, functional and biomarker improvement. Both cellular hypertrophy and diffuse fibrosis are plastic, whereas focal replacement fibrosis is irreversible.

ADDRESS FOR CORRESPONDENCE: Dr. James C. Moon, Barts Heart Centre, St. Bartholomew's Hospital, 2nd Floor, King George V Block, London EC1A 7BE, United Kingdom. E-mail: james.moon@bartshealth.nhs.uk.

PERSPECTIVES

COMPETENCY IN MEDICAL KNOWLEDGE: In patients with AS, myocardial hypertrophy and diffuse fibrosis regress during the first year after AVR, whereas focal fibrosis is relatively irreversible.

TRANSLATIONAL OUTLOOK: Further research should be conducted to develop matrix-modulating therapies that prevent the development of irreversible focal fibrosis.

REFERENCES

- Nkomo VT, Gardin JM, Skelton TN, Gottdiener JS, Scott CG, Enriquez-Sarano M. Burden of valvular heart diseases: a population-based study. *Lancet* 2006;368:1005-11.
- Houser SR, Margulies KB, Murphy AM, et al. Animal models of heart failure: a scientific statement from the American Heart Association. *Circ Res* 2012;111:131-50.
- Azevedo CF, Nigri M, Higuchi ML, et al. Prognostic significance of myocardial fibrosis quantification by histopathology and magnetic resonance imaging in patients with severe aortic valve disease. *J Am Coll Cardiol* 2010;56:278-87.
- Dweck MR, Joshi S, Murigu T, et al. Midwall fibrosis is an independent predictor of mortality in patients with aortic stenosis. *J Am Coll Cardiol* 2011;58:1271-9.
- Barone-Rochette G, Pierard S, De Meester de Ravenstein C, et al. Prognostic significance of LGE by CMR in aortic stenosis patients undergoing valve replacement. *J Am Coll Cardiol* 2014;64:144-54.
- Weidemann F, Herrmann S, Stork S, et al. Impact of myocardial fibrosis in patients with symptomatic severe aortic stenosis. *Circulation* 2009;120:577-84.
- Herrmann S, Stork S, Niemann M, et al. Low-gradient aortic valve stenosis myocardial fibrosis and its influence on function and outcome. *J Am Coll Cardiol* 2011;58:402-12.
- Yarbrough WM, Mukherjee R, Ikonomidis JS, Zile MR, Spinale FG. Myocardial remodeling with aortic stenosis and after aortic valve replacement: mechanisms and future prognostic implications. *J Thorac Cardiovasc Surg* 2012;143:656-64.
- Lim E, Ali A, Theodorou P, et al. Longitudinal study of the profile and predictors of left ventricular mass regression after stentless aortic valve replacement. *Ann Thorac Surg* 2008;85:2026-9.
- Beach JM, Mihaljevic T, Rajeswaran J, et al. Ventricular hypertrophy and left atrial dilatation persist and are associated with reduced survival after valve replacement for aortic stenosis. *J Thorac Cardiovasc Surg* 2014;147:362-9.e8.
- Lamb HJ, Beyerbach HP, de Roos A, et al. Left ventricular remodeling early after aortic valve replacement: differential effects on diastolic function in aortic valve stenosis and aortic regurgitation. *J Am Coll Cardiol* 2002;40:2182-8.
- Pinto AR, Ilinykh A, Ivey MJ, et al. Revisiting cardiac cellular composition. *Circ Res* 2016;118:400-9.
- Maestrini V, Treibel TA, White SK, Fontana M, Moon JC. T1 mapping for characterization of intracellular and extracellular myocardial diseases in heart failure. *Curr Cardiovasc Imaging Rep* 2014;7:9287.
- Flett AS, Hayward MP, Ashworth MT, et al. Equilibrium contrast cardiovascular magnetic resonance for the measurement of diffuse myocardial fibrosis: preliminary validation in humans. *Circulation* 2010;122:138-44.
- Cioffi G, Faggiano P, Vizzardi E, et al. Prognostic effect of inappropriately high left ventricular mass in asymptomatic severe aortic stenosis. *Heart* 2011;97:301-7.
- Ali A, Patel A, Ali Z, et al. Enhanced left ventricular mass regression after aortic valve replacement in patients with aortic stenosis is associated with improved long-term survival. *J Thorac Cardiovasc Surg* 2011;142:285-91.
- Mihaljevic T, Nowicki ER, Rajeswaran J, et al. Survival after valve replacement for aortic stenosis: implications for decision making. *J Thorac Cardiovasc Surg* 2008;135:1270-8; discussion 1278-9.
- Nadjiri J, Nieberler H, Hendrich E, et al. Prognostic value of T1-mapping in TAVR patients: extra-cellular volume as a possible predictor for peri- and post-TAVR adverse events. *Int J Cardiovasc Imaging* 2016;32:1625-33.
- Chin CW, Everett RJ, Kwicinski J, et al. Myocardial fibrosis and cardiac decompensation in aortic stenosis. *J Am Coll Cardiol* 2016;10:1320-33.
- Schwarz F, Flameng W, Schaper J, et al. Myocardial structure and function in patients with aortic valve disease and their relation to post-operative results. *Am J Cardiol* 1978;41:661-9.
- Villari B, Vassalli G, Monrad ES, Chiariello M, Turina M, Hess OM. Normalization of diastolic dysfunction in aortic stenosis late after valve replacement. *Circulation* 1995;91:2353-8.
- Castillo-Moreno JA, Garcia-Escribano IA, Martinez-Pascual-de-Riquelme M, et al. Prognostic usefulness of the 6-minute walk test in patients with severe aortic stenosis. *Am J Cardiol* 2016;118:1239-43.
- Baumgartner H, Hung J, Bermejo J, et al. Echocardiographic assessment of valve stenosis: EAE/ASE recommendations for clinical practice. *Eur J Echocardiogr* 2009;10:1-25.
- Kellman P, Arai AE, Xue H. T1 and extracellular volume mapping in the heart: estimation of error maps and the influence of noise on precision. *J Cardiovasc Magn Reson* 2013;15:56.
- Maceira AM, Prasad SK, Khan M, Pennell DJ. Normalized left ventricular systolic and diastolic function by steady state free precession cardiovascular magnetic resonance. *J Cardiovasc Magn Reson* 2006;8:417-26.

26. Moon JC, Messroghli DR, Kellman P, et al. Myocardial T1 mapping and extracellular volume quantification: a Society for Cardiovascular Magnetic Resonance (SCMR) and CMR Working Group of the European Society of Cardiology consensus statement. *J Cardiovasc Magn Reson* 2013;15:92.
27. Treibel TA, Fontana M, Gilbertson JA, et al. Occult transthyretin cardiac amyloid in severe calcific aortic stenosis: prevalence and prognosis in patients undergoing surgical aortic valve replacement. *Circ Cardiovasc Imaging* 2016;9:e005066.
28. Krayenbuehl HP, Hess OM, Monrad ES, Schneider J, Mall G, Turina M. Left ventricular myocardial structure in aortic valve disease before, intermediate, and late after aortic valve replacement. *Circulation* 1989;79:744-55.
29. Hess OM, Ritter M, Schneider J, Grimm J, Turina M, Krayenbuehl HP. Diastolic stiffness and myocardial structure in aortic valve disease before and after valve replacement. *Circulation* 1984;69:855-65.
30. Flett AS, Sado DM, Quarta G, et al. Diffuse myocardial fibrosis in severe aortic stenosis: an equilibrium contrast cardiovascular magnetic resonance study. *Eur Heart J Cardiovasc Imaging* 2012;13:819-26.
31. Jalil JE, Doering CW, Janicki JS, Pick R, Shroff SG, Weber KT. Fibrillar collagen and myocardial stiffness in the intact hypertrophied rat left ventricle. *Circ Res* 1989;64:1041-50.
32. Treibel TA, López B, González A, et al. Reappraising myocardial fibrosis in severe aortic stenosis: an invasive and non-invasive study in 133 patients. *Eur Heart J* 2017 Jul 22 [E-pub ahead of print].
33. Devereux RB, Devereux RB, Dahlöf B, et al. Regression of hypertensive left ventricular hypertrophy by losartan compared with atenolol: the Losartan Intervention for Endpoint Reduction in Hypertension (LIFE) trial. *Circulation* 2004;110:1456-62.
34. Dahl JS, Videbaek L, Poulsen MK, et al. Effect of candesartan treatment on left ventricular remodeling after aortic valve replacement for aortic stenosis. *Am J Cardiol* 2010;106:713-9.
35. Bull S, Loudon M, Francis JM, et al. A prospective, double-blind, randomized controlled trial of the angiotensin-converting enzyme inhibitor Ramipril In Aortic Stenosis (RIAS trial). *Eur Heart J Cardiovasc Imaging* 2015;16:834-41.
36. Butler J, Fonarow GC, Gheorghide M. Strategies and opportunities for drug development in heart failure. *JAMA* 2013;309:1593-4.
37. Fairbairn TA, Steadman CD, Mather AN, et al. Assessment of valve haemodynamics, reverse ventricular remodelling and myocardial fibrosis following transcatheter aortic valve implantation compared to surgical aortic valve replacement: a cardiovascular magnetic resonance study. *Heart* 2013;99:1185-91.
38. Swynghedauw B. Molecular mechanisms of myocardial remodeling. *Physiol Rev* 1999;79:215-62.
39. Weber KT, Sun Y, Bhattacharya SK, Ahokas RA, Gerling IC. Myofibroblast-mediated mechanisms of pathological remodelling of the heart. *Nat Rev Cardiol* 2013;10:15-26.
40. Singh A, Greenwood JP, Berry C, et al. Comparison of exercise testing and CMR measured myocardial perfusion reserve for predicting outcome in asymptomatic aortic stenosis: the PRognostic Importance of Mlcrovascular Dysfunction in Aortic Stenosis (PRIMID AS) Study. *Eur Heart J* 2017;38:1222-9.
41. Nishimura RA, Otto CM, Bonow RO, et al. 2014 AHA/ACC guideline for the management of patients with valvular heart disease: executive summary: a report of the American College of Cardiology/American Heart Association Task Force on Practice Guidelines. *J Am Coll Cardiol* 2014;63:2438-88.
42. Lindman BR, Stewart WJ, Pibarot P, et al. Early regression of severe left ventricular hypertrophy after transcatheter aortic valve replacement is associated with decreased hospitalizations. *J Am Coll Cardiol Intv* 2014;7:662-73.
43. Monrad ES, Monrad ES, Hess OM, et al. Time course of regression of left ventricular hypertrophy after aortic valve replacement. *Circulation* 1988;77:1345-55.
44. Mahmod M, Piechnik SK, Levelt E, et al. Adenosine stress native T1 mapping in severe aortic stenosis: evidence for a role of the intravascular compartment on myocardial T1 values. *J Cardiovasc Magn Reson* 2014;16:92.
45. Rakusan K, Flanagan MF, Geva T, Southern J, Van Praagh R. Morphometry of human coronary capillaries during normal growth and the effect of age in left ventricular pressure-overload hypertrophy. *Circulation* 1992;86:38-46.
46. Laine GA, Allen SJ. Left ventricular myocardial edema: lymph flow, interstitial fibrosis, and cardiac function. *Circ Res* 1991;68:1713-21.
47. Kellman P, Wilson JR, Xue H, et al. Extracellular volume fraction mapping in the myocardium, part 2: initial clinical experience. *J Cardiovasc Magn Reson* 2012;14:64.
48. McDiarmid AK, Swoboda PP, Erhayem B, et al. Athletic cardiac adaptation in males is a consequence of elevated myocyte mass. *Circ Cardiovasc Imaging* 2016;9:e003579.

KEY WORDS aortic stenosis, fibrosis, left ventricular hypertrophy

APPENDIX For a supplemental Methods section as well as supplemental references, figures, and tables, please see the online version of this article.